11th ANKARA INTERNATIONAL AEROSPACE CONFERENCE **AIAC-2021-174**
8-10 September 2021 - METU, Ankara TURKEY

STRAKE AERODYNAMICS SHAPE OPTIMIZATION IN DOUBLE-DELTA WING CONFIGURATION

Kaan YUTUK* and Alp TIKENOGULLARI†
METU
Ankara, Turkey

Ismail H. TUNCER‡
METU
Ankara, Turkey

ABSTRACT

Modern fighter aircraft mandatorily demands high maneuverability capabilities, and it means well aerodynamics performance in high angles of attack. Naturally, wing of these aircraft is in the form of delta shape and it forms vortex, which creates a suction zone on the wing as a result aerodynamic efficiency increases. In modern aircraft delta shape wings are commonly used with strake to increase performance as a result design of strakes is significant problem. In this study, an optimization study for strake shape design is presented. With this study, optimum shape of the strake for double delta-wing configuration is indicated under certain flight conditions by using adjoint based gradients and free-form deformation method, and it's effects on flow field around configuration with CFD solver, SU^2.

INTRODUCTION

Delta wings are commonly used in aircraft to respond the high maneuverability demands due to their high lift capability. The highly swept, delta, wing notion dated back to the early 1930s. After potential use of delta wings was demonstrated [Polhamus, 1971], the effects of leading-edge vortices on the flow field took more attention. In the following decades, numerous studies explained leading-edge vortex and vortex breakdown behavior on delta wings. To improve the performance of delta wings at high angles, in other words, improve the $C_{L_{max}}$ and corresponding angle of attack, strakes have been researched extensively since the 1970s [Kuchemann, 1978; Rao and Campbell, 1971; Schultz and Flack, 2002]. Wing strakes (also named as "glove", "apex", "leading-edge extension (LEX)" or delta strake-wing configuration known as "double-delta wing") is the forward additional aerodynamic surfaces which are located at the root of the wing in front of the wing leading edge [Nikolic, 2005].

In the literature, many studies investigate the effect of geometric parameters, such as strake span, sweep angle, dihedral, and planform shape [Luckring, 1979; Lamar, 1980; Peake and Tobak, 1983; Lamar and Fink, 1982]. However, LEXs may cause pitch-up tendencies and performance losses as well. Therefore, designing the optimum shape and layout of the strake-wing configuration that

*MSc. Student, Aerospace Engineering Department and Research Engineer, Turkish Aerospace, Email: yutuk.kaan@metu.edu.tr
†MSc. Student, Aerospace Engineering Department, Email: alp.tikenogullari@metu.edu.tr
‡Professor, Aerospace Engineering Department, Email: ismail.h.tuncer@ae.metu.edu.tr

results in the best flight performance at required flight conditions becomes essential. The vortical flow on the strake for the F-18 HARV at low speeds and angles of attack up to $50circ$ is described in the paper by Del Frate et al [Frate, J.H., & Zuniga, F.A. , 1990], which includes surface and off-surface flow graphics and comprehensive pressure distributions. The numerical studies using the Euler and RANS equations to describe flow fields discovered that the intersection of the strake and wing of a flat double delta wing has significant impacts on vortical trajectories and breakdown [kern1992numerical, 1992]. As a result, it has an impact on the wing's aerodynamic performance. Therefore, aerodynamics shape optimization can give the solution to find the best interaction of strake and wing under certain circumstances.

This study aims at solving a gradient-based optimization problem with adjoint method [Economon and et al., 2017] for a double-delta wing configuration and performing a planform shape optimization, numerically, of a strake at a given flight condition. The discrete adjoint methodology is used to obtaining sensitivity values of surfaces as so gradient values [Palacios and et al., 2014] during aerodynamics shape optimization process. On the other hand, for the parametrization of geometry and defining design variables, free-form deformation box technique is used.

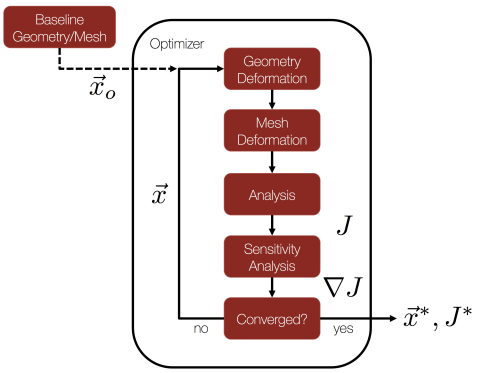

Figure 1: Optimization Cycle [Palacios and et al., 2014]

METHOD

In general, SU^2 is a unique package that is capable of solving PDE systems on a domain [Palacios and et al., 2014]. Any PDE system of a physical model for a particular problem can be represented as following structure:

$$\frac{\partial U}{\partial t} + \Delta \cdot \vec{F}^c(U) - \Delta \cdot \vec{F}^v(U) = Q \quad in\ \Omega \tag{1}$$

U : Vector of state variables
$\vec{F}^c(U)$: Convective fluxes
$\vec{F}^v(U)$: Viscous fluxes
$Q(U)$: Generic source term

Eq.(1) represents a baseline PDE system. However, in this study, an aerodynamic body is a subject governed by the steady-state, compressible RANS equations. The solution domain, which is described with the RANS equations is solved by `SU2_CFD` module, that is one of the module in the SU^2 suite developed in the Aerospace Design Lab at Stanford University [Palacios and et al., 2014]. However, comparison of base and optimum strake geometry Moreover, the SU^2 suite provides an optimization framework (see Figure 1), which involves adjoint solver, `SU2_CFD_AD`, and gradient projection code,

SU2_DOT, that calculates gradients by performing dot products operation between sensitivities and design variables ,and surface deformation utility, as well as optimizer within sciPy.

In the SU^2, to evaluate sensitivities both the discrete and continuous methods are implemented but the discrete adjoint approach is used in the present study. The sensitivity of the numerical residual revaluation with respect to a defined parameter α can be written as:

$$\frac{R}{\alpha} = \frac{\partial R}{\partial U}\frac{dU}{d\alpha} + \frac{\partial U}{\partial \alpha} = 0 \tag{2}$$

rearranging the equation with respect to $\frac{dU}{d\alpha}$ gives:

$$\frac{dU}{d\alpha} = -\left(\frac{\partial R}{\partial U}\right)^{-} 1\frac{\partial R}{\partial \alpha} \tag{3}$$

Let J be the sensitivity of the objective function and it can be expressed in a similar way,

$$\frac{dJ}{d\alpha} = \frac{\partial J}{\partial U}\frac{dU}{d\alpha} + \frac{\partial J}{\partial \alpha} \tag{4}$$

The implementation of Eq. 2.20 in to Eq. 2.21 gives,

$$\frac{dJ}{d\alpha} = -\frac{\partial J}{\partial U}\left(\frac{\partial R}{\partial U}\right)^{-} 1\frac{\partial R}{\partial \alpha} + \frac{\partial J}{\partial \alpha} \tag{5}$$

Finally, The adjoint equation can be expressed as:

$$\left(\frac{\partial R}{\partial U}\right)^{T} \Psi = -\left(\frac{\partial J}{\partial U}\right)^{T} \tag{6}$$

In this method, a matrix called adjoint matrix, Ψ, is computed by solving the above equation (Eq. 2.22). Consequently, the gradient value of the objective function can be written as:

$$\frac{dJ}{d\alpha} = \Psi^{T}\frac{\partial R}{\partial \alpha} + \frac{\partial J}{\partial \alpha} \tag{7}$$

One has to solve the linear system for each objective function. Unlike the finite difference method, in the adjoint method, the cost increases with only the number of the objective function. In the aerodynamics optimization problems, there are a couple of objective functions and different numbers of design variables.

In the present optimization study, aerodynamic efficiency C_L/C_D was selected as an objective function to improve strake wing interaction with computational techniques. Pointwise mesh generation software is used to create grids. Design variables for the optimization cycle are specified with the Free-Form Deformation Box (FFD-Box) technique (see Figure 2). Each node around the FFD-Box is a design variable,and movement of these nodes creates deformation on the shape of the strake.

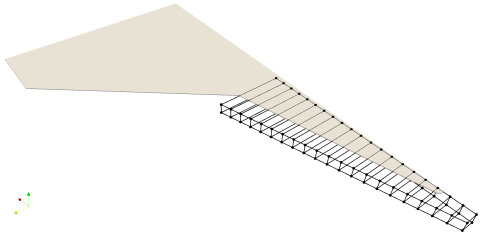

Figure 2: FFD Box

VALIDATION STUDY

Verhaagen et al. state that leading-edge sweep angle and the difference between strake and wing leading edge sweep angles have substantial impacts on vortex interactions and its' breakdowns in the high angle of attack aerodynamics [Verhaagen and et al., 2002]. In the previous studies, high sweep angles, for example, 80°, 76° and 60°, was frequently investigated. Below the 10° angle of attack there is narrow vortex interaction between strake and wing vortices. On the other hand, interactions are enhancing with the increase of angle of attack depending on the leading edge sweep angle. Verhaagen et al., in their experiment, focused on similar highly swept which has 76°- 40° delta strake-wing configuration. Their experiment was investigated with SU^2 RANS solver. The solutions were obtained to research the solver and examine the flow. Solutions are obtained at a Mach number of 0.2, 10° angle of attack and $Re = 1x10^6$ conditions. The model used in the experiment was taken as a basis and in this study is shown in Figure 3.

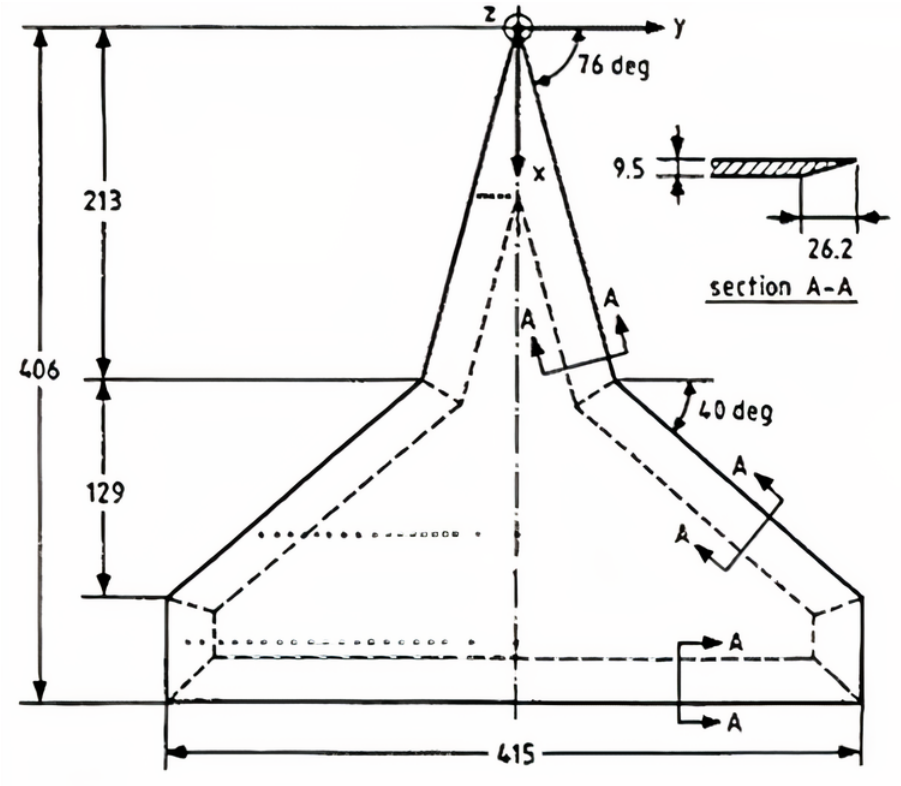

Figure 3: Model of the Validation Geometry [Verhaagen and et al., 2002]

Before obtaining delta strake-wing configuration flow solutions and optimization studies, several grids with different resolutions were generated. Computational grids were created by using Pointwise software with the procedure given in the Methodology section.

The sample of the RANS grid produced by Pointwise software and surface mesh which is created with t-rex technique at leading and trailing edge is given in the Figure 4. Three different grids were generated by controlling the growth ratio of the edges which are 1.1, 1.2, and 1.3 in the surface normal direction. The sample grids with boundary layer mesh are also presented in Figure 5.

After mesh adaptation was executed, a sufficient grid density increase was obtained around the body. Figure 6 shows the grid difference between the based grid and the adapted grid. Therefore, grid statics can be found in Table 1 for the three different boundary layer resolutions and adapted grid.

The computational grids of different resolutions and adapted grids were solved to indicate adequate accuracy is obtained concerning literature. In Figure 7 and Figure 8, comparisons of grids with numerical solutions of the experiment and literature are given. Especially as can be seen in Figure 8, as a result of the comparison between "coarse", "medium" and "fine" grids, the higher the

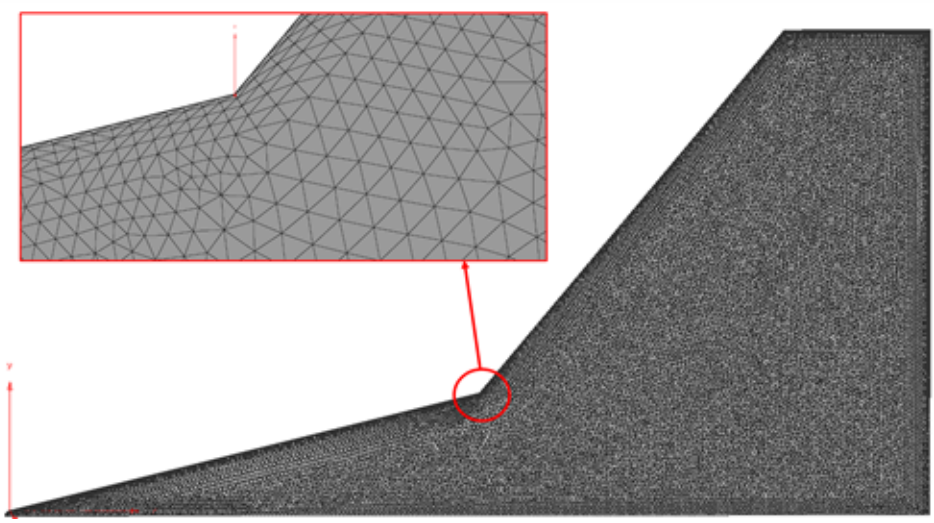

Figure 4: Surface Mesh on Top of Strake-Wing Geometry

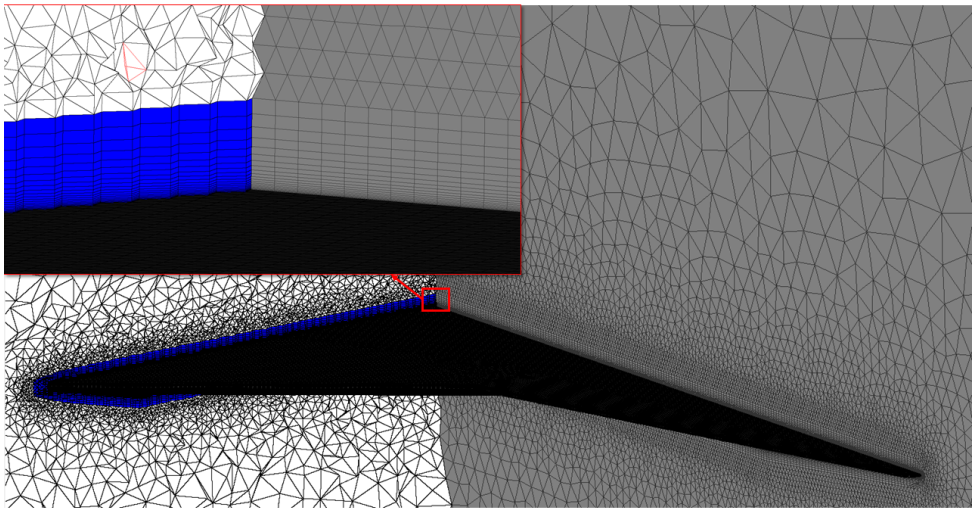

Figure 5: Volume Mesh of Strake-Wing Geometry

Mesh Metrics	
Mesh	Number of Nodes
Course Mesh	800K
Middle Mesh	1.1M
Fine Mesh	1.6M
Adapted Mesh	1.3M

Table 1: Mesh Sizes Used in Mesh Independency Study

resolution, the higher the strength of the strake and wing eddies. Likewise, as the resolution at 75% cord increases, the region with a low pressure coefficient value at 55% of the wingspan is calculated more accurately. When the number of cells and pressure coefficient distribution of the grids with "medium" and "fine" resolution were compared, it was decided to achieve the final grid resolution by adapting over the "medium" grid because the calculations were close to each other. As can be seen in Figure 8, the adapted "medium" solution grid gives more sensitive results in the region with the lowest pressure coefficient value and in the vortex regions with the maximum negative pressure

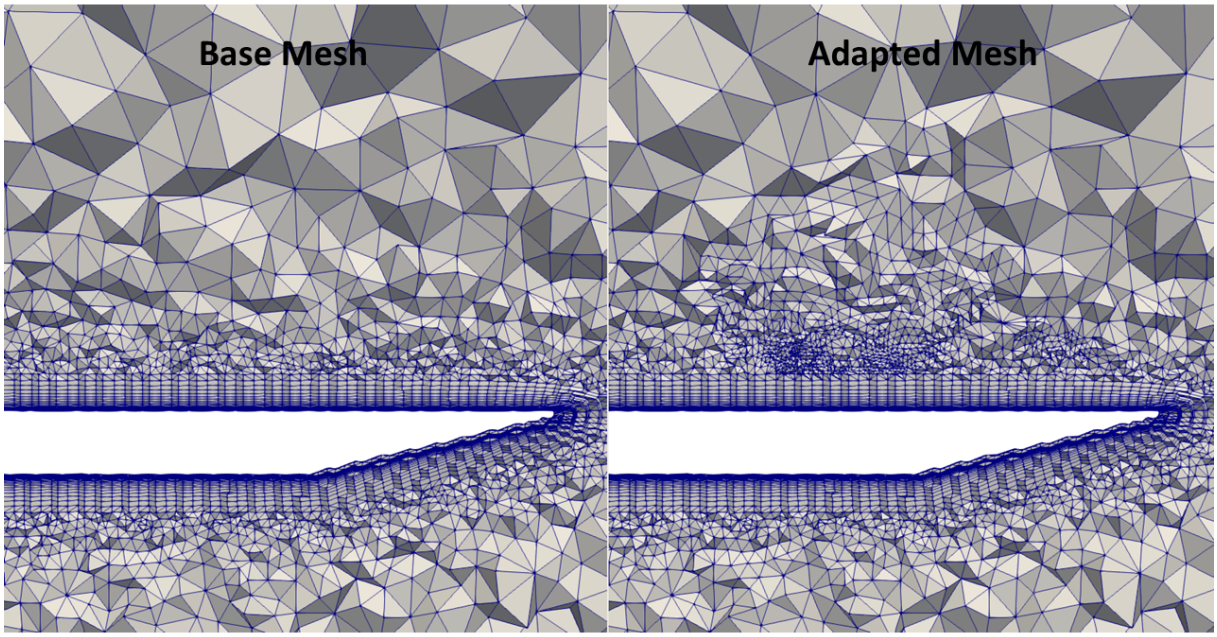

Figure 6: Comparison of Adapted Mesh and Base Mesh of Strake-Wing Geometry

coefficient value.

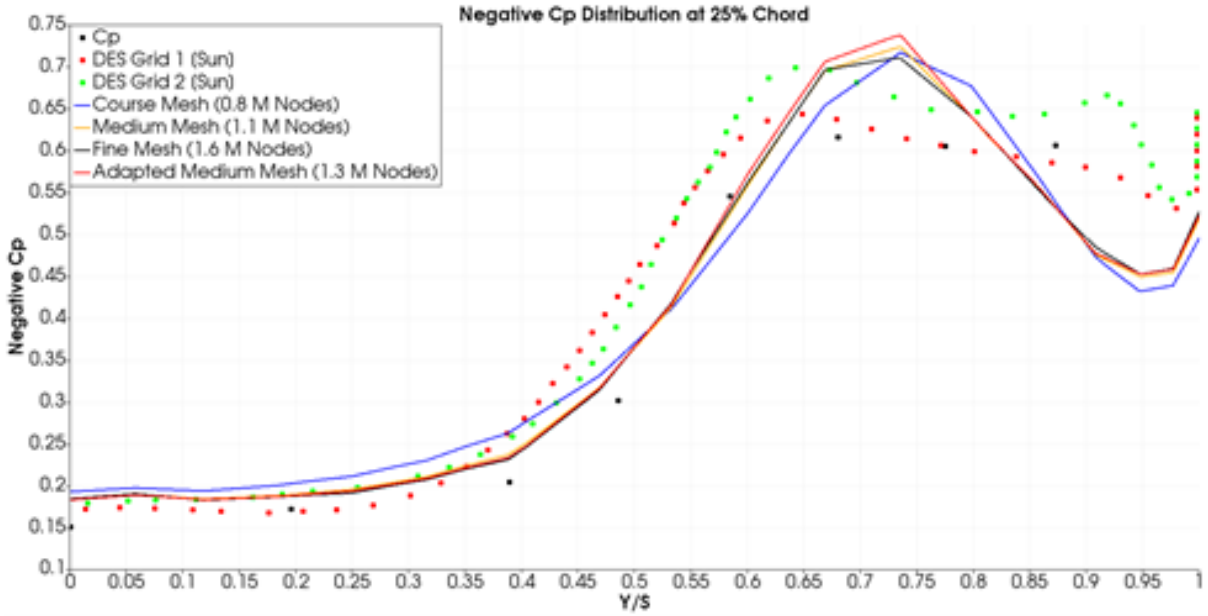

Figure 7: Comparison of Pressure Coefficient Values on Surface For Different Meshes along Span at 25% of Chord

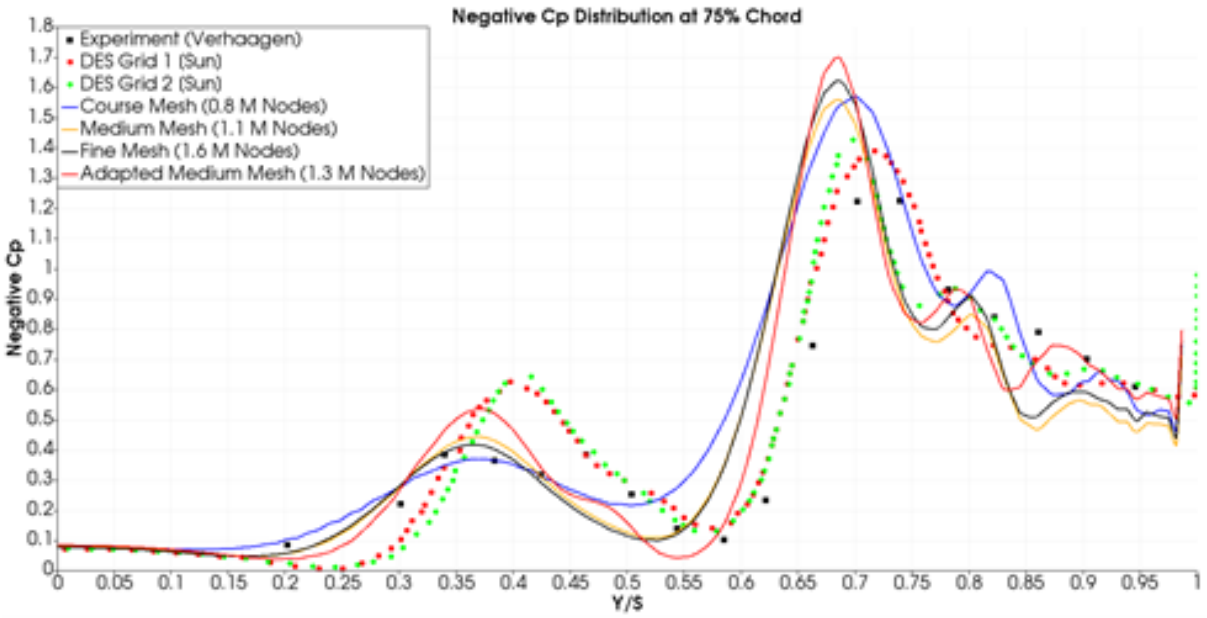

Figure 8: Comparison of Pressure Coefficient Values on Surface For Different Meshes along Span at 75% of Chord

RESULTS AND DISCUSSION

In this section, result of shape optimization of strake geometry is performed and investigated for 10° angle of attack. The optimization process was initiated from Verhaagen's [Verhaagen and et al., 2002] delta strake design. However, by optimizing the shape of the strake geometry, gothic strake design with a higher aerodynamic efficiency is obtained from this delta strake at the specified angle of attack and mach conditions.

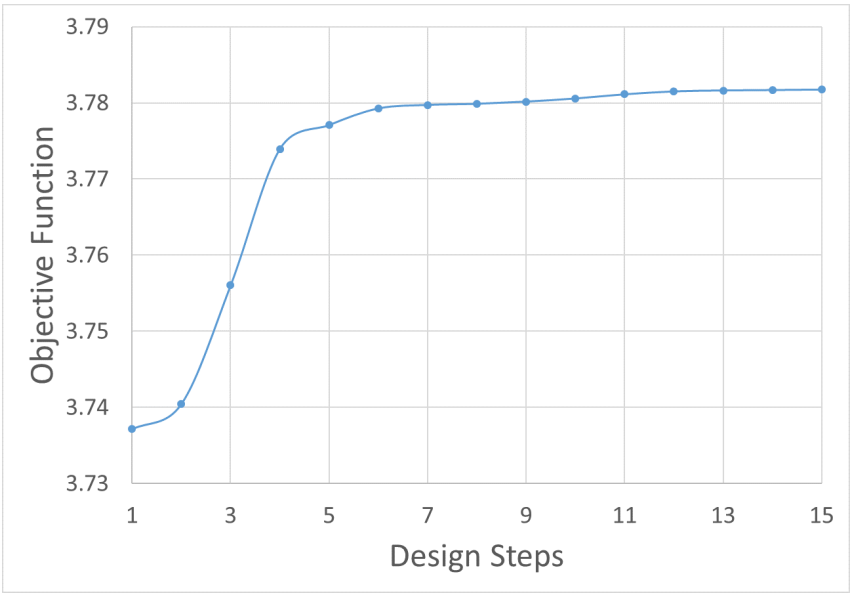

Figure 9: Change of Aerodynamics Efficiency with Design Steps During Shape Optimization at AoA = 10

The changes in the objective function and planform shapes during the shape optimization process are shown in Figure 9 and Figure 10. As can be seen, the planform shape has changed greatly in the first six design steps, and the objective function has also greatly increased in the first six steps.

After the 6th design step, the deformations are especially concentrated in front of the kink point. Shape optimization provides about 1% more improvement in the objective function at the 10° angle of attack. In addition, optimized and base designs have similar planform areas.

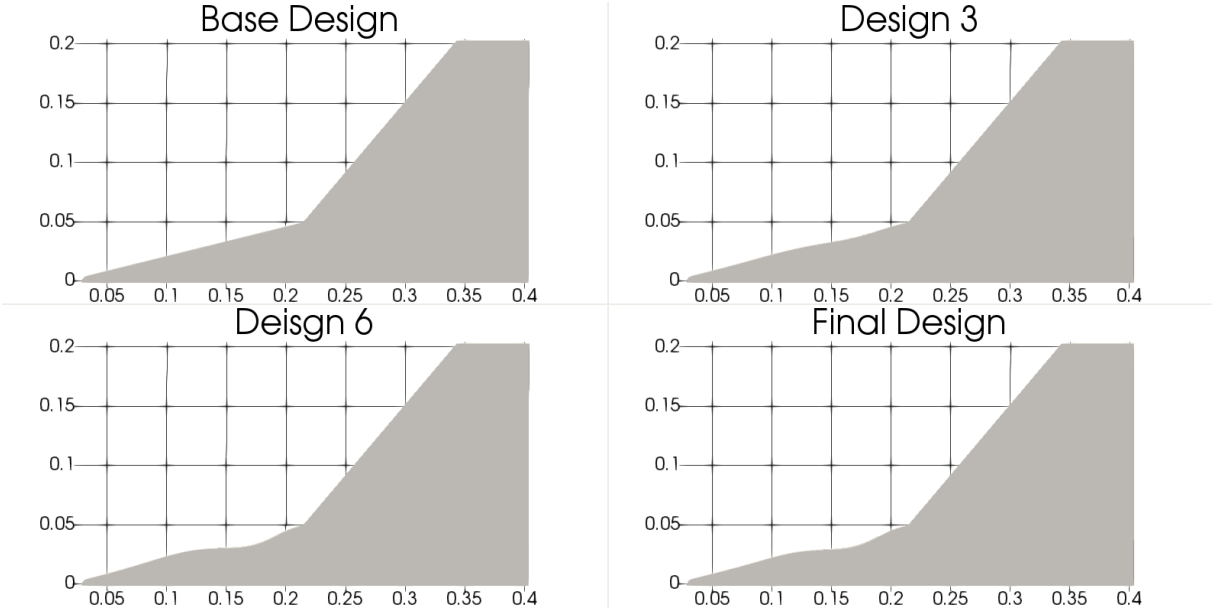

Figure 10: Change of Strake Design with Design Steps During Shape Optimization at AoA = 10

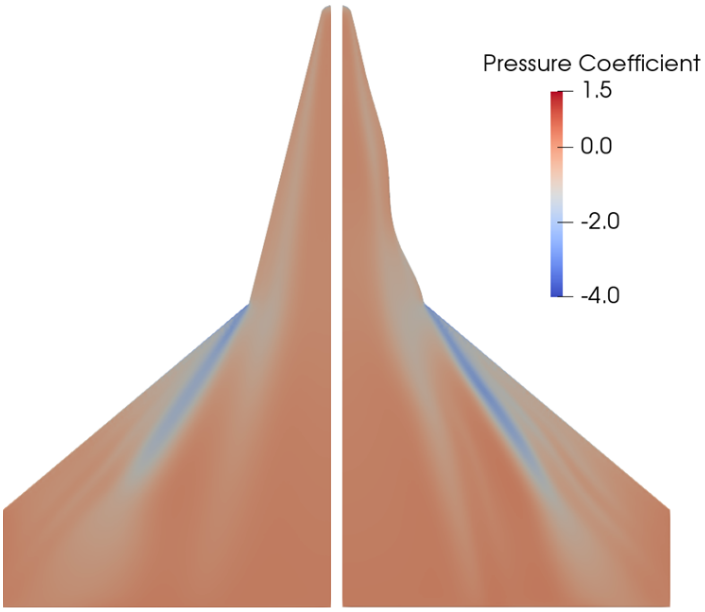

Figure 11: Comparison of Surface Pressure Distribution between Base and Shape Optimized Geometries at AoA = 10

Figure 11 and Figure 12 show surface pressure distributions and surface pressure at cross-sections along with wing vortex core streamlines at a 10° angle of attack. When the effects of strake and wing vortices on the surface pressure distributions are compared in both designs, it is seen that the optimization process changes the vortex strength. Especially in optimum design, the effect of the

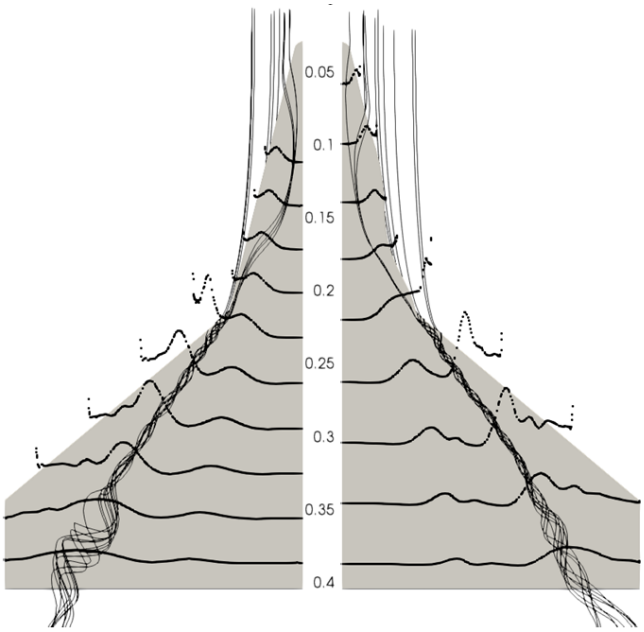

Figure 12: Illustration of Streamlines along Wing Vortex and Pressure Plots for Base and Shape Optimized Geometries at AoA = 10

wing vortex on the surface pressure is remarkable. When Figure 12 is examined, it is seen that the optimized design makes the wing vortex more regular than the basic design, similar to the planform optimization study at the same angle of attack. In addition, wing vortex initiates with more powerful suction at the kink point with respect to based design. However, Figure 12 is also pointed out the effect of the strake vortex on the surface has decreased.

For the investigation of the interaction of vortices, Q-criteria is a powerful tool. Figure 13 indicates results supporting the surface pressure view. For the optimized geometry, two different strake vortices existence can be seen because of the gothic shape of the strake, and the second strake vortex near the kink point forms through a bit inboard. The first strake vortex increases the strength of the second vortex by swirling around it and these vortices merge downstream. This affects the formation and existence of the wing vortex. Unlike based design, strake vortex goes without a breakdown and this structure helps to wing vortex preserves its energy a bit longer. In addition, depending on the strake vortex's existence, a counter-rotating separation vortex is noticeable near the strake vortex.

In contrast to the two vortex movements indicated in the Q-criteria image in Figure 13, Figure 14 shows that the velocities in the vortex centers move in a close pattern along the entire vortex line. However, upon closer inspection, it is seen that the non-dimensional velocity in the vortex center drops below 0, around 85% of the wing chord length in the base design. In this region, a reverse pressure gradient was formed due to vortex breakdown. This effect was not seen in the optimized design. This statement supports the vortex breakdown effect seen in the q-criteria image. Furthermore, when the non-dimensional velocity is examined along the wing, it is also seen that the velocity at the center of the vortex is always higher in the optimized design.

CONCLUSION

In this study, shape optimization of strake-wing configuration is performed by using the open-source CFD toolkit, SU^2. During the optimization process, gradient values are obtained by using the discrete adjoint solution of the flow field to achieve an optimum point of aerodynamics efficiency. Aerodynamics shape optimization is performed at 10° and 0.2 M. Increase in aerodynamics efficiency

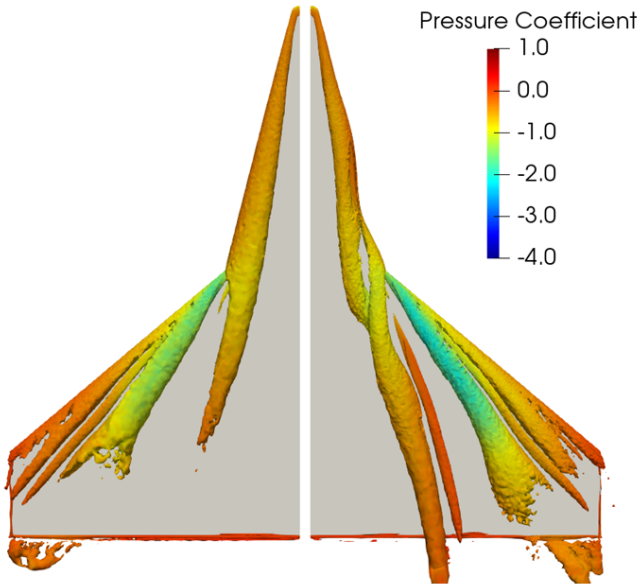

Figure 13: Illustration of Q-criteria with Pressure Coefficient for Base and Shape Optimized Geometries at AoA = 10

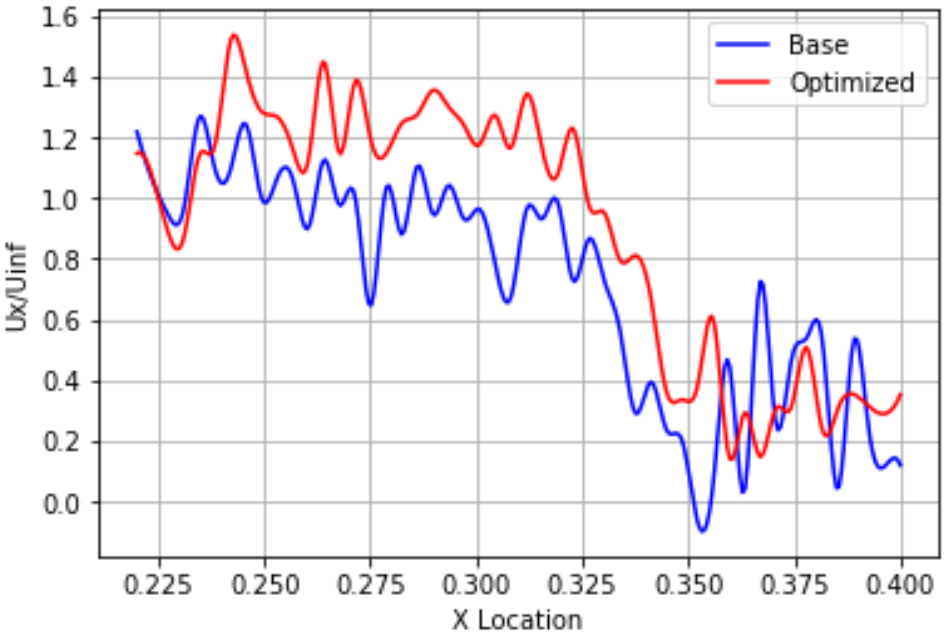

Figure 14: Comparison of Non-Dimensionalized Axial Velocity to Free-Stream Along Wing Chord Line for Base and Shape Optimized Geometries at AoA = 10

is limited with %1 in the optimum point of shape optimization study. By optimum design of strake geometry, stronger wing vortex is obtained and vortex breakdown is delayed in this study.

References

Economon, T. D., Alonso, J. J., Albring, T. A., & Gauger, N. R. (2017). *Adjoint formulation investigations of benchmark aerodynamic design cases IN SU2.* 35th AIAA Applied Aerodynamics Conference. doi:10.2514/6.2017-4363

Küchemann, D. (1978). *The aerodynamic design of aircraft a detailed introduction. to the current aerodynamic knowledge and pract. guide to the solution of aircraft design problems.* Oxford, NY, Toronto, Sydney, Paris, Kronberg/Taunus: Pergamon Press.

Lamar, J. E. (1980). *Analysis and design of strake-wing configurations.* Journal of Aircraft, 17(1), 20-27. doi:10.2514/3.57870

Lamar, J. E., & Frink, N. T. (1982). *Aerodynamic features of designed strake-wing configurations.* Journal of Aircraft, 19(8), 639-646. doi:10.2514/3.57444

Del Frate, J. O. H. N., & Zuniga, F. (1990). *In-flight flow field analysis on the NASA F-18 High Alpha Research Vehicle with comparisons to ground facility data.* In 28th Aerospace Sciences Meeting (p. 231).

Luckring, J. M. (1979). *Aerodynamics of Strake-Wing Interactions.* Journal of Aircraft, 16(11), 756-762. doi:10.2514/3.58600

Nikolic, V. R. (2005). *Movable tip strakes and wing aerodyanmics.* Journal of Aircraft, 42(6), 1418-1426. doi:10.2514/1.4615

Palacios, F., Economon, T. D., Aranake, A., Copeland, S. R., Lonkar, A. K., Lukaczyk, T. W., . . . Alonso, J. J. (2014). *Stanford University Unstructured (SU2): Analysis and design technology for turbulent flows.* 52nd Aerospace Sciences Meeting. doi:10.2514/6.2014-0243

Peake, D. J., & Tobak, M. (1983, June). *On issues concerning flow separation and vortical flows in 3 dimensions.* Retrieved April 10, 2021, from https://ntrs.nasa.gov/

Kern, S. (1992). *A numerical investigation of vortex flow control through small geometry modifications at the strake/wing junction of a cropped double-delta wing.* In 30th Aerospace Sciences Meeting and Exhibit (p. 411).

Polhamus, E. C. (1971). *Predictions of vortex-lift characteristics by a leading-edge suction analogy.* Journal of Aircraft, 8(4), 193-199. doi:10.2514/3.44254

Rao, D. M., & Campbell, J. F. (1987). *Vortical flow management techniques.* Progress in Aerospace Sciences, 24(3), 173-224. doi:10.1016/0376-0421(87)90007-8

Schultz, M. P., & Flack, K. A. (2002). *Effect of Strake geometry and Centerbody on the lift of swept wings.* Journal of Aircraft, 39(2), 377-379. doi:10.2514/2.2938

Verhaagen, N., Jenkins, L., Kern, S., & Washburn, A. (1995). *A study of the vortex flow over a 76/40-deg Double-delta wing.* 33rd Aerospace Sciences Meeting and Exhibit. doi:10.2514/6.1995-650